

# Quantum Phases of Time Order in Many-Body Ground States

Tie-Cheng Guo<sup>1,\*</sup> and Li You<sup>1,2,†</sup>

<sup>1</sup>*State Key Laboratory of Low Dimensional Quantum Physics,  
Department of Physics, Tsinghua University, Beijing 100084, China*

<sup>2</sup>*Frontier Science Center for Quantum Information, Beijing, China*

(Dated: April 28, 2021)

Understanding phases of matter is of both fundamental and practical importance. Prior to the widespread appreciation and acceptance of topological order, the paradigm of spontaneous symmetry breaking, formulated along the Landau-Ginzburg-Wilson (LGW) dogma, is central to understanding phases associated with order parameters of distinct symmetries and transitions between phases. This work proposes to identify ground state phases of quantum many-body system in terms of *time order*, which is operationally defined by the appearance of nontrivial temporal structure in the two-time auto-correlation function of a symmetry operator (order parameter). As a special case, the (symmetry protected) *time crystalline order* phase detects continuous time crystal (CTC). Time order phase diagrams for spin-1 atomic Bose-Einstein condensate (BEC) and quantum Rabi model are fully worked out. Besides time crystalline order, the intriguing phase of time functional order is discussed in two non-Hermitian interacting spin models.

A consistent theme for studying many-body system, particularly in condensed matter physics, concerns the classification of phases and their associated phase transitions [1–3]. In the celebrated Landau-Ginzburg-Wilson (LGW) paradigm [4, 5], spontaneous symmetry breaking plays a central role with order parameters characterizing different phases of matter possessing respective broken symmetries. Other schemes for classifying phases as well as their associated transitions are, however, beyond the Landau-Ginzburg-Wilson paradigm, which are by now well accepted since first established decades ago [6–8]. For example, topological order, which classifies gapped quantum many-body system constitutes a topical research direction [7–10]. Our current understanding categories gapped systems into gapped liquid phases [11] and gapped non-liquid phases, with the former broadly including phases of topological order [7, 8], symmetry enriched topological order [12–15], and symmetry protected trivial order [16–18], while the recently discussed fracton phases [19–21] belongs to the latter of gapped non-liquid phases.

Temporal properties of phases are also worthy of investigations as exemplified by many recent studies [22–24]. For instance, time crystal (TC) or perpetual temporal dependence in a many-body ground state that breaks spontaneously time translation symmetry (TTS), constitutes an exciting new phenomenon. First proposed by Wilczek [24] for quantum systems and followed by Shapere and Wilczek [25] for classical systems in 2012, TC in their original sense is unfortunately ruled out by Bruno’s no-go theorem the following year [26, 27]. Watanabe and Oshikawa (WO) reformulate the idea of quantum TC [28], and present a refined no-go theorem for many-body systems without too long-range interactions [28]. Most recent efforts on this topic are directed towards non-equilibrium discrete/Floquet TC breaking discrete TTS [29–34], particularly in systems with disorder that facili-

tate many-body localizations [30, 33], in addition to clean systems [35–38]. Ongoing studies are further extended to open systems with Floquet driving in the presence of dissipation [39–43], with experimental investigations reported for a variety of systems [44–50]. A recent study addresses TC and its associated physics along imaginary time axis [51].

We introduce *time order* in this work, as the essential element for a new perspective to identify and categorize quantum many-body phases, based on different ground state temporal patterns. Each quantum many-body Hamiltonian  $\hat{H}$  comes with its evolution or time translation operator  $e^{-i\hat{H}t}$ . When continuous time translation symmetry is broken for operator  $e^{-i\hat{H}t}$ , akin to the breaking of continuous spatial translation symmetry for operator  $e^{-i\vec{k}\cdot\vec{r}}$ , time crystals arise in direct analogy to spatial crystals [24]. The message we hope to convey here in this study is rooted on the dual between  $\hat{H}$  and  $e^{-i\hat{H}t}$ , which we argue quite generally establishes a solid foundation for time order and provides further information concerning ground state quantum phases based on time domain properties. Different quantum many-body states with the same temporal patterns are classified into the same time order phases, of which continuous TC (CTC), a ground state with periodic time dependence breaking continuous TTS as originally proposed in Refs. [24, 25], belongs to one of them.

We will adopt the WO definition of CTC based on two-time auto-correlation function of an operator. First outlined in the now famous no-go theorem work [28], it establishes a general and rigorous subtype of CTC: the WO CTC. Recently, Kozin and Kyriienko claim to have realized such a genuine ground state CTC in a multi-spin model with long-range interaction [52], buttressing much confidence to the search for exotic CTCs. The operational definition for time order we introduced encompasses WO CTC as one type of time order phases.

We will also explore and elaborate a variety of possible exotic phases.

## RESULTS

### Time order

We argue that ground state temporal properties of a quantum many-body system can be used to characterize or classify its phases. Hence, the concept of *time order* can be introduced analogous to an order parameter by bestowing it in the non-trivial temporal dependence. To exemplify the essence of the associated physics, we shall present an operational definition for *time order* and accordingly work out the exhaustive list of all allowed phases. According to the WO proposal [28], a witness to CTC is the following two-time (or unequal time) auto-correlation function (with respect to ground state)

$$\lim_{V \rightarrow \infty} \langle \hat{\Phi}(t) \hat{\Phi}(0) \rangle / V^2 \equiv f(t), \quad (1)$$

for operator  $\hat{\Phi}(t) \equiv \int_V d^D x \hat{\phi}(\vec{x}, t)$  defined as an integrated order parameter (over  $D$ -spatial-dimension), or analogously the volume averaged one,

$$f(t) = \lim_{V \rightarrow \infty} \langle \hat{\phi}(t) \hat{\phi}(0) \rangle, \quad (2)$$

with  $\hat{\phi}(\vec{x}, t)$  the corresponding local order parameter density operator  $\hat{\phi} \equiv \hat{\Phi}/V$ .

If  $f(t)$  is time periodic, the system is in a state of CTC. This can be reformulated into an explicit operational protocol by introducing twisted vector. *For a quantum many-body system with energy eigen-state  $|\psi_i\rangle$ , if there exists a coarse-grained Hermitian order parameter  $\hat{\phi}$ ,  $\hat{\phi}|\psi_i\rangle$  is called the eigen-state twisted vector; More generally, if  $\hat{\phi}$  is non-Hermitian,  $\hat{\phi}|\psi_i\rangle$  (or  $\hat{\phi}^\dagger|\psi_i\rangle$ ) will be called the right (or left) eigen-state twisted vector.*

The orthonormal set of eigen-wavefunctions  $|\psi_i\rangle$  ( $i = 0, 1, 2, \dots$ ) for a system described by Hamiltonian  $\hat{H}$  is arranged in increasing eigen-energies  $\epsilon_i$  with  $i = 0$  denoting the ground state. When the coarse-grained order parameter  $\hat{\phi}$  is Hermitian, the ground state twisted vector  $|v\rangle$  can be expanded  $|v\rangle \equiv \hat{\phi}(0)|\psi_0\rangle = \sum_{i=0}^{\infty} a_i |\psi_i\rangle$  into the eigen-basis. With the help of the Schrödinger equation  $i\partial|\psi(t)\rangle/\partial t = \hat{H}|\psi(t)\rangle$  ( $\hbar = 1$  assumed throughout) for the system wave function  $|\psi(t)\rangle$ , we obtain

$$\begin{aligned} f(t) &= \lim_{V \rightarrow \infty} \langle \psi_0 | e^{i\hat{H}t} \hat{\phi}(0) e^{-i\hat{H}t} \hat{\phi}(0) | \psi_0 \rangle \\ &= \lim_{V \rightarrow \infty} e^{i\epsilon_0 t} \langle v | e^{-i\hat{H}t} | v \rangle \\ &= \lim_{V \rightarrow \infty} \sum_{j=0}^{\infty} \eta_j e^{-i(\epsilon_j - \epsilon_0)t}, \end{aligned} \quad (3)$$

where  $\eta_j \equiv |a_j|^2$  denote weights of the ground state twisted vector,  $\eta_0$  the corresponding ground state weight, and  $\eta_j$  (with  $j > 0$ ) the excited state weight.

When the coarse-grained order parameter  $\hat{\phi}$  is non-Hermitian, we use  $|v^{(l)}\rangle$  and  $|v^{(r)}\rangle$  to denote respectively the left and right ground state twisted vectors and expand them analogously in the eigen-basis to arrive at  $|v^{(l)}\rangle \equiv \hat{\phi}^\dagger|\psi_0\rangle = \sum_{i=0}^{\infty} b_i |\psi_i\rangle$  and  $|v^{(r)}\rangle \equiv \hat{\phi}|\psi_0\rangle = \sum_{i=0}^{\infty} a_i |\psi_i\rangle$ . In this case, we find

$$\begin{aligned} f(t) &= \lim_{V \rightarrow \infty} \langle \psi_0 | e^{i\hat{H}t} \hat{\phi}(0) e^{-i\hat{H}t} \hat{\phi}(0) | \psi_0 \rangle \\ &= \lim_{V \rightarrow \infty} e^{i\epsilon_0 t} \langle v^{(l)} | e^{-i\hat{H}t} | v^{(r)} \rangle \\ &= \lim_{V \rightarrow \infty} \sum_{j=0}^{\infty} \eta_j e^{-i(\epsilon_j - \epsilon_0)t}, \end{aligned} \quad (4)$$

with  $\eta_j \equiv b_j^* a_j$  weights of the ground state twisted vector instead. Similarly  $\eta_0$  and  $\eta_j$  ( $j > 0$ ) denote respectively ground and excited state weights.

Given an order parameter  $\hat{\phi}$ , quite generally  $f(t)$  is a sum of many harmonic functions with amplitudes  $\eta_j$  and characteristic frequencies  $\omega_j \equiv \epsilon_j - \epsilon_0$ . Nontrivial time dependence of the two-time auto-correlation function is thus imbedded in the energy spectra of  $H$  as well as in the weights of the ground state twisted vector. For CTC order to exist, one of the excited state weights must be non-vanishing, or in rare cases,  $f(t)$  can include harmonic terms of commensurate frequencies.

If  $f(t)$  is a constant, the time dependence will be trivial. However, a subtlety appears when  $f(t)$  is vanishingly small with respect to system size. Since what we are after is the system's explicit temporal behavior or time dependence, which is easily washed out to  $f(t) = 0$  by a vanishing norm of the twisted vector. Such a difficulty can be mitigated by multiplying system volume  $V$ , *i.e.*, using the twisted vector  $|v\rangle \rightarrow V|v\rangle$  to check if the correlation for the bulk order parameter  $F(t) \equiv V^2 f(t)$  exhibits temporal dependence, or vanishes.

$$F(t) = \lim_{V \rightarrow \infty} \langle \hat{\Phi}(t) \hat{\Phi}(0) \rangle. \quad (5)$$

When  $f(t) = 0$  but  $F(t)$  remains a periodic function, the system can still be considered a CTC. Such a remedy surprisingly captures the essence of generalized CTC of Ref.[53].

The analysis presented above can be directly extended to excited states [54]. It is also straightforwardly applicable to non-Hermitian systems, as long as a plausible “ground state” can be identified, for example, by requiring its eigen-energy to possess the largest imaginary part or the smallest norm. Denoting the imaginary part of energy eigen-value  $E_i$  as  $\text{Im}(E_i)$ , a prefactor  $\propto e^{\text{Im}(E_i)t}$  then arises in the auto-correlation function, leading to unusual time functional order in the classification of time order.

Therefore, quantum many-body phases can be classified according to *time order*. The two-time auto-correlation function based complete operational procedure for classifying time order thus extends the definition

TABLE I. Classification of the ground state phases for a quantum many-body system

Phase		Property of two-time auto-correlator
Time trivial order		$f(t) = \text{const.} \neq 0$ or $f(t) = 0, F(t) = \text{const.}$
Time order	Time crystalline order	$f(t)$ is periodic and nonvanishing
	Time quasi-crystalline order	$f(t)$ is quasiperiodic with beats from two incommensurate frequencies
	Time functional order	$f(t)$ is aperiodic
	Generalized time crystalline order	$f(t) = 0, F(t)$ is periodic and nonvanishing
	Generalized time quasi-crystalline order	$f(t) = 0, F(t)$ contains beats from two incommensurate frequencies
Generalized time functional order		$f(t) = 0, F(t)$ is aperiodic

of WO CTC in Ref. [28]. Our central results can be simply stated in the following: *If  $f(t)$  exhibits nontrivial time dependence, time order exists. If  $f(t) = 0$ , but  $F(t)$  displays nontrivial time dependence instead, generalized time order exists.*

More specifically, if  $f(t) = \text{const.}$  is nonzero, the system exhibits time trivial order. The same applies when  $f(t) = 0$  and  $F(t) = \text{const.}$ . For all other situations, nontrivial time order prevails. A complete classification for all time order ground state phases is shown in Table I, according to the temporal behaviors of their auto-correlation functions  $f(t)$  or  $F(t)$ . As shown in the Supplementary Material (SM), the above discussion and classification on time order can be extended to finite temperature systems as well.

The operational procedure outlined above presents a straightforward approach for detecting *time order*, albeit with reference to an order parameter operator. Hence more appropriately, this approach should be called *order parameter assisted time order* or *symmetry-based (or -protected) time order*, to emphasize its reference to symmetry order parameter of a quantum many-body system. The twisted vector facilitates easy calculations to distinguish between different time order phases from time trivial ones, as we illustrate below in terms of a few concrete examples. It is reasonable to expect that transitions between different time order phases can occur, reminiscent of phase transitions in the LGW spontaneous symmetry breaking paradigm.

### Time order phase in a spin-1 atomic condensate

A spin-1 atomic Bose-Einstein condensate (BEC) under single spatial mode approximation (SMA) [55–57] is described by the following Hamiltonian

$$\hat{H} = \frac{c_2}{2N} \left[ (2\hat{N}_0 - 1) (\hat{N} - \hat{N}_0) + 2 (\hat{a}_1^\dagger \hat{a}_{-1}^\dagger \hat{a}_0 \hat{a}_0 + \text{h.c.}) \right] - p (\hat{N}_1 - \hat{N}_{-1}) + q (\hat{N}_1 + \hat{N}_{-1}), \quad (6)$$

where  $\hat{a}_{m_F}$  ( $m_F = 0, \pm 1$ ) ( $\hat{a}_{m_F}^\dagger$ ) denotes the annihilation (creation) operator for atom in the ground state

Zeeman manifold  $|F = 1, m_F\rangle$  with corresponding number operator  $\hat{N}_{m_F} = \hat{a}_{m_F}^\dagger \hat{a}_{m_F}$ . The total atom number  $\hat{N} = \hat{N}_1 + \hat{N}_0 + \hat{N}_{-1}$  is conserved.  $p$  and  $q$  are linear and quadratic Zeeman shifts that can be tuned independently [58], while  $c_2$  describes the strength of spin exchange interaction.

The validity of this model is well established based on extensive theoretical [59–62] and experimental [58, 63–65] studies of spinor BEC over the years. The fractional population in spin states  $|1, 1\rangle$  and  $|1, -1\rangle$ ,  $\hat{n}_{\text{sum}} \equiv N_{\text{sum}}/N$ , with  $N_{\text{sum}} = \hat{N}_1 + \hat{N}_{-1} = N - N_0$ , is often chosen as an order parameter [62, 64, 66, 67] with  $N$  assuming the role of system size. The ground state twisted vector then becomes  $|\nu\rangle \equiv \hat{n}_{\text{sum}}|\psi_0\rangle$ , and

$$f(t) = \lim_{N \rightarrow \infty} \langle \hat{n}_{\text{sum}}(t) \hat{n}_{\text{sum}}(0) \rangle, \quad (7)$$

$$F(t) = \lim_{N \rightarrow \infty} \langle \hat{N}_{\text{sum}}(t) \hat{N}_{\text{sum}}(0) \rangle. \quad (8)$$

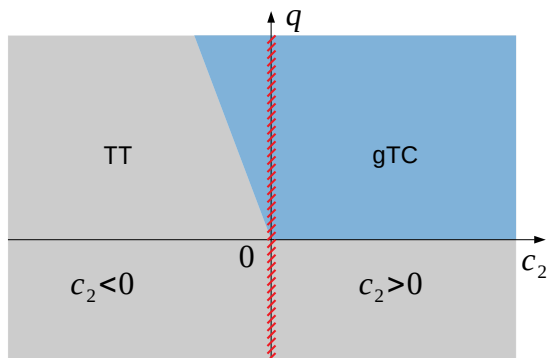


FIG. 1. Time order phase diagram for spin-1 atomic BEC, where TT and gTC respectively denote time trivial and generalized time crystalline order. The region of (hashed) line segments surrounding  $c_2 = 0$  for noninteracting system is to be excluded.

We will concentrate on the zero magnetization  $F_z = 0$  subspace and employ exact diagonalization (ED) to calculate eigen-states.  $p = 0$  is assumed since  $F_z$  is conserved. Figure 1 illustrates the system's complete time order phase diagram. For ferromagnetic interaction  $c_2 <$

0 as with  $^{87}\text{Rb}$  atoms, the critical quadratic Zeeman shift  $q/|c_2| = 2$  splits the whole region into time trivial order (TT) phase for smaller  $q$  that observes TTS, and generalized time crystalline (gTC) order phase for  $q/|c_2| > 2$  where TTS is spontaneously broken. The latter (gTC phase) is found to coincide with the polar phase [62]. Limited by available computation resources, the system sizes we explored with ED remain moderate which prevent us from mapping out the finer details in the immediate neighborhood of  $q = 2|c_2|$ . Further elaboration of time order properties in this region is therefore needed. On the other hand, for antiferromagnetic interaction  $c_2 > 0$  with  $^{23}\text{Na}$  atoms, we find  $q = 0$  separates TT phase from gTC order. We note here that  $q = 2|c_2|$  is the second-order quantum phase transition (QPT) critical point between the polar phase and the broken-axisymmetry phase of the ferromagnetic spin-1 BEC, while  $q = 0$  corresponds to the first-order QPT critical point for antiferromagnetic interaction.

More detailed discussions including the dependence of time order phases on system size, possible approaches to detect them, and extension to thermal state phases can be found in the SM.

### Time order phase diagram for quantum Rabi model

As a second example, we consider time order phases of the quantum Rabi model described by the Hamiltonian

$$\hat{H}_{\text{Rabi}} = \omega_0 \hat{a}^\dagger \hat{a} + \frac{\Omega}{2} \hat{\sigma}_z - \lambda (\hat{a} + \hat{a}^\dagger) \hat{\sigma}_x, \quad (9)$$

where  $\hat{\sigma}_{x,z}$  is Pauli matrix of a two-level system (transition frequency  $\Omega$ ),  $\hat{a}(\hat{a}^\dagger)$  is the annihilation (creation) operator for a single bosonic field mode (of frequency  $\omega_0$ ), and  $\lambda$  is their coupling strength.

It is known that the above model exhibits a QPT to a superradiant state, despite of its simplicity [68]. The transition occurs at the critical point  $g_c \equiv 1$ , with the dimensionless parameter  $g \equiv 2\lambda/\sqrt{\omega_0\Omega}$ . The equivalent thermodynamic limit is approached by taking  $\Omega/\omega_0 \rightarrow \infty$ . According to the studies in Ref. [68], an almost exact effective low-energy Hamiltonian for the normal phase ( $g < 1$ ) is given by

$$\hat{H}_{\text{np}} = \omega_0 \hat{a}^\dagger \hat{a} - \frac{\omega_0 g^2}{4} (\hat{a} + \hat{a}^\dagger)^2 - \frac{\Omega}{2}, \quad (10)$$

whose low-energy eigen-states are  $|\phi_{\text{np}}^m(g)\rangle = \hat{\mathcal{S}}[r_{\text{np}}(g)]|m\rangle|\downarrow\rangle$  for  $g \leq 1$ , with  $\hat{\mathcal{S}}[x] = \exp[x(\hat{a}^{\dagger 2} - \hat{a}^2)/2]$  and  $r_{\text{np}}(g) = -[\ln(1 - g^2)]/4$ , and the energy eigen-values are  $E_{\text{np}}^m(g) = m\epsilon_{\text{np}}(g) + E_{\text{G,np}}(g)$ , with  $\epsilon_{\text{np}}(g) = \omega_0\sqrt{1 - g^2}$  and  $E_{\text{G,np}}(g) = [\epsilon_{\text{np}}(g) - \omega_0]/2 - \Omega/2$ . For the superradiant phase ( $g > 1$ ), the effective low energy Hamiltonian becomes

$$\hat{H}_{\text{sp}} = \omega_0 \hat{a}^\dagger \hat{a} - \frac{\omega_0}{4g^4} (\hat{a} + \hat{a}^\dagger)^2 - \frac{\Omega}{4} (g^2 + g^{-2}), \quad (11)$$

whose eigen-states are given by  $|\phi_{\text{sp}}^m(g)\rangle_{\pm} = \hat{\mathcal{D}}[\pm\alpha_g] \hat{\mathcal{S}}[r_{\text{sp}}(g)]|m\rangle|\downarrow^{\pm}\rangle$ , with  $r_{\text{sp}}(g) = -[\ln(1 - g^{-4})]/4$ ,  $\alpha_g = \sqrt{(\Omega/4g^2\omega_0)(g^4 - 1)}$ , and  $\hat{\mathcal{D}}[\alpha] = e^{\alpha(\hat{a}^\dagger - \hat{a})}$ . The displacement-dependent spin states are  $|\downarrow^{\pm}\rangle = \mp\sqrt{(1 - g^{-2})/2}|\uparrow\rangle + \sqrt{(1 + g^{-2})/2}|\downarrow\rangle$ , while the energy eigen-values take the form  $E_{\text{sp}}^m(g) = m\epsilon_{\text{sp}}(g) + E_{\text{G,sp}}(g)$ , with  $\epsilon_{\text{sp}}(g) = \omega_0\sqrt{1 - g^{-4}}$  and  $E_{\text{G,sp}}(g) = [\epsilon_{\text{sp}}(g) - \omega_0]/2 - \Omega(g^2 + g^{-2})/4$ . More details can be found in the SM of Ref. [68].

For this model, the scaled average cavity photon number  $\hat{n}_c = \omega_0 \hat{a}^\dagger \hat{a} / \Omega$  is a suitable order parameter with  $\Omega/\omega_0$  assuming the role of system size. The corresponding bulk order parameter then becomes  $\hat{N}_c = \hat{a}^\dagger \hat{a}$  or the average cavity photon number, and

$$f(t) = \lim_{\Omega/\omega_0 \rightarrow \infty} \langle \hat{n}_c(t) \hat{n}_c(0) \rangle, \quad (12)$$

$$F(t) = \lim_{\Omega/\omega_0 \rightarrow \infty} \langle \hat{N}_c(t) \hat{N}_c(0) \rangle.$$

For  $g < 1$ , we find

$$f(t) = 0, \quad (13)$$

$$F(t) = \eta_0 + \eta_2 e^{-i(2\epsilon_{\text{np}})t},$$

respectively, where  $\eta_0 = \sinh^4(r_{\text{np}})$  and  $\eta_2 = \cosh^2(r_{\text{np}}) \sinh^2(r_{\text{np}})$ . For  $g > 1$ , we obtain

$$f(t) = \frac{(g^2 - g^{-2})^2}{16}. \quad (14)$$

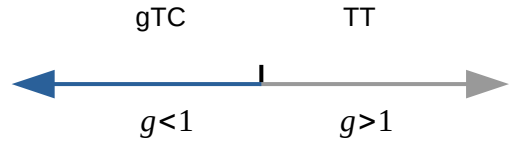


FIG. 2. Time order phase diagram for the quantum Rabi model, where TT and gTC respectively denote time trivial and generalized time crystalline order.

The time order phase diagram is shown in Fig. 2. When  $g < 1$ , the system ground state corresponds to a generalized time crystalline order phase, while the system exhibits time trivial order when  $g > 1$ . Despite of such a simple model composed of a two-level system and a bosonic field mode, the ground state of the quantum Rabi model displays intriguing temporal phase structure accompanied by a finite-component quantum phase transition.

### Non-Hermitian many-body interaction model

Finally we consider two effective models with many-body spin-spin interaction and non-Hermitian effects.

The first is described by Hamiltonian

$$\hat{H} = -\frac{1}{N(N-1)} \sum_{1 \leq i < j \leq N} (\lambda + i\gamma) \sigma_1^x \sigma_2^x \cdots \sigma_i^y \cdots \sigma_j^y \cdots \sigma_N^x, \quad (15)$$

with two  $\sigma^y$  operators at sites  $i$  and  $j$  in a string of otherwise  $\sigma^x$   $N$ -body spin interaction.  $1/[N(N-1)]$  is the normalization factor,  $\lambda$  is the spin interaction strength, and  $\gamma$  represents an effective dissipation rate.  $\lambda > 0$  and  $\gamma \geq 0$  are both real numbers.

We observe that the Greenberger-Horne-Zeilinger (GHZ) states

$$|G_{\pm}\rangle = \frac{1}{\sqrt{2}}(|0\rangle^{\otimes N} \pm |1\rangle^{\otimes N}) \quad (16)$$

correspond to two nondegenerate system eigen-states with eigen-energies  $\pm(\lambda + i\gamma)/2$ . The spectra of this model system is bounded inside the circle of radius  $\sqrt{\lambda^2 + \gamma^2}/2$  in the complex plane. The eigen-state whose eigen-value has the largest imaginary part is taken as the ground state, or  $|GS\rangle = |G_+\rangle$  with eigen-energy  $\epsilon_0 = (\lambda + i\gamma)/2$ . The highest excited state is  $|G_-\rangle$ , whose corresponding eigen-energy is  $\epsilon_{2N-1} = -(\lambda + i\gamma)/2$ .

An appropriate order parameter operator in this case becomes the average magnetization  $\hat{m} = \sum_{i=1}^N \sigma_i^z/N$ . The twisted vector becomes  $|v\rangle = \hat{m}|GS\rangle = |G_-\rangle$ , and the auto-correlator can be easily worked out to be  $f(t) = \lim_{N \rightarrow \infty} \langle \hat{m}(t) \hat{m}(0) \rangle = e^{-i\lambda t} e^{\gamma t}$ . When  $\gamma = 0$ , the system ground state exists time-crystalline order phase and corresponds to a continuous time crystal [52]. When  $\gamma \neq 0$ , the system exhibits time functional order, with an exploding  $f(t)$  as time evolves.

A second non-Hermitian model Hamiltonian is given by

$$\hat{H} = (\lambda + i\gamma) \left( \sigma_1^x \sigma_2^x \cdots \sigma_{[N/2]}^x - \sigma_{[N/2]+1}^x \cdots \sigma_N^x \right) - \sum_{j=1}^N \sigma_j^z \sigma_{j+1}^z, \quad (17)$$

where  $[ \cdot ]$  denotes the integer part,  $\sigma_{N+1} \equiv \sigma_1$  corresponds to the periodic boundary condition,  $\lambda$  and  $\gamma$  are spin-string interaction strength and dissipation strength respectively as in the previous model, both of them are real. This Hamiltonian contains  $[(N+1)/2]$ -body interaction terms and supports GHZ state  $|G_+\rangle$  as a non-degenerate excited state [69] with eigen-energy  $\epsilon_+ = -N$ . The other two eigen-states of concern are  $|\Psi^{\pm}\rangle \equiv (\alpha_1 |G_-\rangle + \alpha_2 |\tilde{G}_{-, \mathcal{I}}\rangle) / \sqrt{|\alpha_1|^2 + |\alpha_2|^2}$  with  $\alpha_1 = 1$  and  $\alpha_2 = -(N + \epsilon^{\pm})/2(\lambda + i\gamma)$ , where

$$|\tilde{G}_{-, \mathcal{I}}\rangle = \frac{1}{\sqrt{2}} (|0\rangle_1 \cdots |0\rangle_{[N/2]} |1\rangle_{[N/2]+1} \cdots |1\rangle_N - |1\rangle_1 \cdots |1\rangle_{[N/2]} |0\rangle_{[N/2]+1} \cdots |0\rangle_N). \quad (18)$$

The eigen-energies for  $|\Psi^{\pm}\rangle$  are given by  $\epsilon^{\pm} = -N + 2 \pm 2\sqrt{1 + (\lambda + i\gamma)^2}$ , with more details of the derivation given in SM. For the same order parameter operator  $\hat{m}$ , we find  $\hat{m}|\Psi_0\rangle \xrightarrow{N \rightarrow \infty} \alpha_1 |G_+\rangle / \sqrt{|\alpha_1|^2 + |\alpha_2|^2}$ .

At  $\gamma = 0$ , the above non-Hermitian Hamiltonian (17) reduces to a Hermitian one, whose ground state  $|\Psi_0\rangle$  corresponds to the one with smaller  $\epsilon$  from  $|\Psi^{(-)}\rangle$  and  $|\Psi^{(+)}\rangle$ , or  $\epsilon_0 = -N - 2(\sqrt{1 + \lambda^2} - 1)$ . The ground state  $|\Psi_0\rangle$  for this non-Hermitian system is therefore chosen from  $|\Psi^{(-)}\rangle$  or  $|\Psi^{(+)}\rangle$  to be the one that deforms into the right Hermitian case one when  $\gamma$  approaches zero. However, the criteria for the ground state energy  $\epsilon_0$  corresponds to choosing the smaller one from  $\epsilon^{\pm}$  when  $\epsilon$  is real and choosing the one with the larger imaginary part when  $\epsilon$  is complex.

Therefore we directly obtain

$$f(t) = \lim_{N \rightarrow \infty} \langle \hat{m}(t) \hat{m}(0) \rangle = \frac{|\alpha_1|^2}{|\alpha_1|^2 + |\alpha_2|^2} e^{-i(\epsilon_+ - \epsilon_0)t}. \quad (19)$$

When  $\lambda \neq 0$  and  $\gamma \neq 0$ , the system exists in *time functional order phase*, again results from the non-Hermitian Hamiltonian. When  $\lambda \neq 0$  but  $\gamma = 0$ , the auto-correlation function reduces to

$$f(t) = \frac{1}{2} \left( 1 + \frac{1}{\sqrt{1 + \lambda^2}} \right) e^{-2i(\sqrt{1 + \lambda^2} - 1)t}, \quad (20)$$

as for a genuine time crystal of the WO type exhibiting time crystalline order. When  $\lambda = 0$  and  $0 < |\gamma| \leq 1$ , we find

$$f(t) = \frac{1}{2} (1 + \sqrt{1 - \gamma^2}) e^{-2i(\sqrt{1 - \gamma^2} - 1)t}. \quad (21)$$

The system ground state again exhibits time-crystalline order. When  $\lambda = 0$  and  $|\gamma| > 1$ , we obtain

$$f(t) = \frac{1}{2} e^{2it} e^{-2\sqrt{\gamma^2 - 1}t}, \quad (22)$$

by choosing  $\epsilon_0 = -N + 2 + 2i\sqrt{\gamma^2 - 1}$  as the ground state eigen-energy from the two eigen-values  $-N + 2 \pm 2i\sqrt{\gamma^2 - 1}$ . The system ground state now exhibits time functional order phase, with a decaying  $f(t)$  as time evolves. When  $\lambda = \gamma = 0$ ,

$$f(t) = 1, \quad (23)$$

the ground state reduces to time trivial order phase.

The above two non-Hermitian models represent direct generalizations of the Hermitian system considered in Refs. [52, 69]. While slightly more complicated, they remain sufficient simple for compact analytical treatment, thus helping to reveal interesting and clear physical meanings of the underline time order.

### Some remarks about continuous time crystal

According to the WO no-go theorem [28],  $f(t)$  for the ground state or the Gibbs ensemble of a general many-body Hamiltonian whose interactions are not-too-long ranged exhibits no temporal dependence, hence belongs to time trivial order according to our classification scheme. At first sight, this seems to sweep many important models of condensed matter physics into the same boring class of time trivial order phase. However, it remains to explore, for instance, many-body systems with more than two-body (or  $k$ -body) interactions, or non-Hermitian systems, which might support the existence of CTC. Inspired by the recent results on CTC [52], we believe more time crystalline phases will be uncovered and further understanding will be gained in the future.

As emphasized earlier, continuous time crystal results from spontaneously breaking continuous time translation symmetry. Due to the genuine time periodicity contained in CTC, it might be possible to explore and design *new types of clocks* based on macroscopic many-body systems, as the time period is directly related to energy spectra, and whose physical meaning is clearly the same as for atomic clock states. Furthermore, they are not affected by finite size effect in contrast to periodicity in DTC.

## DISCUSSION

While ground state phases of a quantum many-body system are mostly classified with its Hamiltonian based on two paradigms: LGW symmetry breaking order parameter or topological order, this work proposes to study phases from time dimension using *time order* or more specifically with the proposed symmetry-based time order. Compared to the recent progress and understanding gained for topological order [9, 10], one could try to develop a framework for *entanglement-based time order* instead of the *symmetry-based time order* we employ here in this study. Quantum entanglement in a many-body system is responsible for topological order, whose origin lies at the tensor product structure of the quantum many-body Hilbert space  $\mathcal{H}_{\text{tot}} = \otimes_i \mathcal{H}_i$  with  $\mathcal{H}_i$  the finite-dimensional Hilbert space for site- $i$ . An *entanglement-based time order* therefore calls for a combined investigation to exploit quantum entanglement and temporal properties of a quantum many-body system.

Through *time order*, one focuses on temporal structure of the evolution operator  $e^{-i\hat{H}t}$ . The *symmetry-based time order* therefore unifies LGW paradigm with the concept of *time order*, while an *entanglement-based time order* could amalgamate topological order paradigm (or entanglement beyond that) with time order. For this to happen, a more basic definition for *time order* will be required, which will likely expand into further in-depth

investigations.

In conclusion, understanding phases of matter constitutes a corner stone of contemporary physics. Capitalizing on the concept of CTC for many body ground state with perpetual time dependence, this study argues that information from time domain can be employed to classify quantum phase as well, which provides a new perspective towards the understanding of ground state time dependence, significantly beyond existing studies on CTC. We introduce time order, provide its operational definition in terms of two-time auto-correlation function of an appropriate symmetry order operator, bestow physical meaning to characteristic frequencies and amplitudes of the correlation function, and present complete classification of time order phases. Time order phase diagrams for a spin-1 BEC system and the quantum Rabi model are fully worked out. Interesting time order phases in non-Hermitian spin models with multi-body interaction are presented. Besides the time crystalline order which already attracts broad attention from its studies in terms of CTC, other phases we identify, e.g. time quasi-crystalline order and time functional order, represent exciting new possibilities.

## METHODS

The Supplementary Material contains all calculation details. In Sec. I we extend the discussion of time order to finite temperature where concrete examples in spin-1 BEC system are given. In Sec. II we present the numerical method for studying the spin-1 BEC example, while in Sec. III we provide the variational result about the polar ground state of a spin-1 BEC. In Sec. IV we show details about the ground state calculation in the non-Hermitian quantum many-body models considered.

## ACKNOWLEDGMENTS

This work is supported by the National Key R&D Program of China (Grant No. 2018YFA0306504), and by the National Natural Science Foundation of China (NSFC) (Grants No. 11654001 and No. U1930201), and by the Key-Area Research and Development Program of Guangdong Province (Grant No. 2019B030330001).

## AUTHOR CONTRIBUTIONS

T.-C.G. proposed and conducted the research, supervised by L.Y.; T.-C.G. and L.Y. discussed the results and wrote the manuscript.

## CODE AVAILABILITY

Source code for generating the plots is available from the authors upon request.

## DATA AVAILABILITY

The data that support the plots within this paper and other findings of this study are available from the corresponding author upon request.

---

\* [gtc16@mails.tsinghua.edu.cn](mailto:gtc16@mails.tsinghua.edu.cn)

† [lyou@mail.tsinghua.edu.cn](mailto:lyou@mail.tsinghua.edu.cn)

- [1] X.-G. Wen, *Quantum Field Theory of Many-Body Systems* (Oxford University Press, 2004).
- [2] E. Fradkin, *Field Theories of Condensed Matter Physics*, 2nd ed. (Oxford University Press, 2004).
- [3] S. Sachdev, *Quantum Phase Transitions* (Cambridge University Press, 1999).
- [4] L. D. Landau and E. Lifshitz, *Statistical Physics* (Butterworth-Heinemann, 1999).
- [5] K. G. Wilson and J. Kogut, *Physics reports* **12**, 75 (1974).
- [6] T. Senthil, A. Vishwanath, L. Balents, S. Sachdev, and M. P. Fisher, *Science* **303**, 1490 (2004).
- [7] X. G. Wen, *Phys. Rev. B* **40**, 7387 (1989).
- [8] X. G. WEN, *International Journal of Modern Physics B* **04**, 239 (1990).
- [9] X.-G. Wen, *Rev. Mod. Phys.* **89**, 041004 (2017).
- [10] X.-G. Wen, *Science* **363**, eaal3099 (2019).
- [11] B. Zeng and X.-G. Wen, *Phys. Rev. B* **91**, 125121 (2015).
- [12] X.-G. Wen, *Phys. Rev. B* **65**, 165113 (2002).
- [13] X. Chen, F. J. Burnell, A. Vishwanath, and L. Fidkowski, *Phys. Rev. X* **5**, 041013 (2015).
- [14] M. Cheng, Z.-C. Gu, S. Jiang, and Y. Qi, *Phys. Rev. B* **96**, 115107 (2017).
- [15] C. Heinrich, F. Burnell, L. Fidkowski, and M. Levin, *Phys. Rev. B* **94**, 235136 (2016).
- [16] Z.-C. Gu and X.-G. Wen, *Phys. Rev. B* **80**, 155131 (2009).
- [17] X. Chen, Z.-X. Liu, and X.-G. Wen, *Phys. Rev. B* **84**, 235141 (2011).
- [18] X. Chen, Z.-C. Gu, Z.-X. Liu, and X.-G. Wen, *Phys. Rev. B* **87**, 155114 (2013).
- [19] W. Shirley, K. Slagle, and X. Chen, *SciPost Phys.* **6**, 15 (2019).
- [20] W. Shirley, K. Slagle, Z. Wang, and X. Chen, *Phys. Rev. X* **8**, 031051 (2018).
- [21] S. Vijay, J. Haah, and L. Fu, *Phys. Rev. B* **94**, 235157 (2016).
- [22] M. Mierzejewski, K. Giergiel, and K. Sacha, *Phys. Rev. B* **96**, 140201 (2017).
- [23] K. Sacha, *Scientific reports* **5**, 10787 (2015).
- [24] F. Wilczek, *Phys. Rev. Lett.* **109**, 160401 (2012).
- [25] A. Shapere and F. Wilczek, *Phys. Rev. Lett.* **109**, 160402 (2012).
- [26] P. Bruno, *Phys. Rev. Lett.* **111**, 070402 (2013).
- [27] P. Nozières, *EPL (Europhysics Letters)* **103**, 57008 (2013).
- [28] H. Watanabe and M. Oshikawa, *Phys. Rev. Lett.* **114**, 251603 (2015).
- [29] K. Sacha, *Phys. Rev. A* **91**, 033617 (2015).
- [30] C. W. von Keyserlingk, V. Khemani, and S. L. Sondhi, *Phys. Rev. B* **94**, 085112 (2016).
- [31] D. V. Else, B. Bauer, and C. Nayak, *Phys. Rev. Lett.* **117**, 090402 (2016).
- [32] V. Khemani, A. Lazarides, R. Moessner, and S. L. Sondhi, *Phys. Rev. Lett.* **116**, 250401 (2016).
- [33] N. Y. Yao, A. C. Potter, I.-D. Potirniche, and A. Vishwanath, *Phys. Rev. Lett.* **118**, 030401 (2017).
- [34] D. V. Else, C. Monroe, C. Nayak, and N. Y. Yao, *Annual Review of Condensed Matter Physics* **11**, 467 (2020).
- [35] A. Russomanno, F. Iemini, M. Dalmonte, and R. Fazio, *Phys. Rev. B* **95**, 214307 (2017).
- [36] B. Huang, Y.-H. Wu, and W. V. Liu, *Phys. Rev. Lett.* **120**, 110603 (2018).
- [37] C.-h. Fan, D. Rossini, H.-X. Zhang, J.-H. Wu, M. Artoni, and G. C. La Rocca, *Phys. Rev. A* **101**, 013417 (2020).
- [38] F. Machado, D. V. Else, G. D. Kahanamoku-Meyer, C. Nayak, and N. Y. Yao, *Phys. Rev. X* **10**, 011043 (2020).
- [39] Z. Gong, R. Hamazaki, and M. Ueda, *Phys. Rev. Lett.* **120**, 040404 (2018).
- [40] F. M. Gambetta, F. Carollo, M. Marcuzzi, J. P. Garrahan, and I. Lesanovsky, *Phys. Rev. Lett.* **122**, 015701 (2019).
- [41] A. Riera-Campeny, M. Moreno-Cardoner, and A. Sanpera, *Quantum* **4**, 270 (2020).
- [42] A. Lazarides, S. Roy, F. Piazza, and R. Moessner, *Phys. Rev. Research* **2**, 022002 (2020).
- [43] J. G. Cosme, J. Skulte, and L. Mathey, *Phys. Rev. A* **100**, 053615 (2019).
- [44] J. Zhang, P. W. Hess, A. Kyprianidis, P. Becker, A. Lee, J. Smith, G. Pagano, I.-D. Potirniche, A. C. Potter, A. Vishwanath, N. Y. Yao, and C. Monroe, *Nature (London)* **543**, 217 (2017).
- [45] S. Choi, J. Choi, R. Landig, G. Kucsko, H. Zhou, J. Isoya, F. Jelezko, S. Onoda, H. Sumiya, V. Khemani, C. von Keyserlingk, N. Y. Yao, E. Demler, and M. D. Lukin, *Nature (London)* **543**, 221 (2017).
- [46] J. Rovny, R. L. Blum, and S. E. Barrett, *Phys. Rev. B* **97**, 184301 (2018).
- [47] J. Rovny, R. L. Blum, and S. E. Barrett, *Phys. Rev. Lett.* **120**, 180603 (2018).
- [48] S. Pal, N. Nishad, T. S. Mahesh, and G. J. Sreejith, *Phys. Rev. Lett.* **120**, 180602 (2018).
- [49] S. Autti, V. B. Eltsov, and G. E. Volovik, *Phys. Rev. Lett.* **120**, 215301 (2018).
- [50] J. Smits, L. Liao, H. T. C. Stoof, and P. van der Straten, *Phys. Rev. Lett.* **121**, 185301 (2018).
- [51] Z. Cai, Y. Huang, and W. V. Liu, *Chinese Physics Letters* **37**, 050503 (2020).
- [52] V. K. Kozin and O. Kyriienko, *Phys. Rev. Lett.* **123**, 210602 (2019).
- [53] M. Medenjak, B. Buča, and D. Jaksch, *Phys. Rev. B* **102**, 041117 (2020).
- [54] A. Syrwid, J. Zakrzewski, and K. Sacha, *Phys. Rev. Lett.* **119**, 250602 (2017).
- [55] C. K. Law, H. Pu, and N. P. Bigelow, *Phys. Rev. Lett.* **81**, 5257 (1998).
- [56] H. Pu, C. K. Law, S. Raghavan, J. H. Eberly, and N. P. Bigelow, *Phys. Rev. A* **60**, 1463 (1999).

- [57] S. Yi, O. E. Müstecaplıođlu, C. P. Sun, and L. You, *Phys. Rev. A* **66**, 011601 (2002).
- [58] X.-Y. Luo, Y.-Q. Zou, L.-N. Wu, Q. Liu, M.-F. Han, M. K. Tey, and L. You, *Science* **355**, 620 (2017).
- [59] M.-S. Chang, Q. Qin, W. Zhang, L. You, and M. S. Chapman, *Nat. Phys.* **1**, 111 (2005).
- [60] W. Zhang, B. Sun, M. Chapman, and L. You, *Phys. Rev. A* **81**, 033602 (2010).
- [61] J. Guzman, G.-B. Jo, A. N. Wenz, K. W. Murch, C. K. Thomas, and D. M. Stamper-Kurn, *Phys. Rev. A* **84**, 063625 (2011).
- [62] M. Xue, S. Yin, and L. You, *Phys. Rev. A* **98**, 013619 (2018).
- [63] M.-S. Chang, C. Hamley, M. Barrett, J. Sauer, K. Fortier, W. Zhang, L. You, and M. Chapman, *Phys. Rev. Lett.* **92**, 140403 (2004).
- [64] M. Anquez, B. A. Robbins, H. M. Bharath, M. Boguslawski, T. M. Hoang, and M. S. Chapman, *Phys. Rev. Lett.* **116**, 155301 (2016).
- [65] L.-Y. Qiu, H.-Y. Liang, Y.-B. Yang, H.-X. Yang, T. Tian, Y. Xu, and L.-M. Duan, *Science Advances* **6**, eaba7292 (2020).
- [66] B. Damski and W. H. Zurek, *Phys. Rev. Lett.* **99**, 130402 (2007).
- [67] A. Lamacraft, *Phys. Rev. Lett.* **98**, 160404 (2007).
- [68] M.-J. Hwang, R. Puebla, and M. B. Plenio, *Phys. Rev. Lett.* **115**, 180404 (2015).
- [69] P. Facchi, G. Florio, S. Pascazio, and F. V. Pepe, *Phys. Rev. Lett.* **107**, 260502 (2011).



# Supplementary Material for “Quantum Phases of Time Order in Many-Body Ground States”

Tie-Cheng Guo<sup>1</sup> and Li You<sup>1,2</sup>

<sup>1</sup>*State Key Laboratory of Low Dimensional Quantum Physics,  
Department of Physics, Tsinghua University, Beijing 100084, China*  
<sup>2</sup>*Frontier Science Center for Quantum Information, Beijing, China*

This supplementary provides supporting material and related details for the presentation of the main text. It is organized as follows: in Sec. I we extend the discussion of time order to finite temperature; in Sec. II, we present calculation details related to the spin-1 atomic Bose-Einstein condensate (BEC) example considered; as a more straightforward approach to understand numerical results, we present a variational approach for treating the polar ground state of a spin-1 BEC in Sec. III. Finally, we give the details about ground state and eigen-energy calculation in the non-Hermitian quantum many-body model with multi-body interaction in Sec. IV.

## I. TIME ORDER AT FINITE TEMPERATURE

At finite temperature  $T$ , excited states will be populated, which can be taken into account with the Gibbs ensemble  $\hat{\rho} \equiv e^{-\beta\hat{H}}/Z$ , where  $Z \equiv \text{Tr} e^{-\beta\hat{H}}$  denotes the partition function and  $\beta \equiv 1/T$  the inverse temperature. We then find

$$\begin{aligned} f(t) &\rightarrow \lim_{V \rightarrow \infty} \text{Tr} \left( e^{i\hat{H}t} \hat{\phi}(0) e^{-i\hat{H}t} \hat{\phi}(0) \hat{\rho} \right) \\ &= \lim_{V \rightarrow \infty} \sum_{k=0}^{\infty} \langle \psi_k | e^{i\hat{H}t} \hat{\phi}(0) e^{-i\hat{H}t} \hat{\phi}(0) \frac{e^{-\beta\hat{H}}}{Z} | \psi_k \rangle \\ &= \lim_{V \rightarrow \infty} \sum_{k=0}^{\infty} \frac{1}{Z} e^{i\epsilon_k t - \beta\epsilon_k} \langle v_k | e^{-i\hat{H}t} | v_k \rangle \\ &= \lim_{V \rightarrow \infty} \sum_{k=0}^{\infty} \sum_{j=0}^{\infty} \frac{1}{Z} c_{jk} e^{-\beta\epsilon_k} e^{-i(\epsilon_j - \epsilon_k)t}, \end{aligned} \quad (1)$$

where  $|v_k\rangle$  is the eigen-state twisted vector for  $|\psi_k\rangle$ , and  $c_{jk}$  its associated weight. Analogously, for the non-Hermitian case, we find

$$\begin{aligned} f(t) &= \lim_{V \rightarrow \infty} \sum_{k=0}^{\infty} \frac{1}{Z} e^{i\epsilon_k t - \beta\epsilon_k} \langle v_k^{(l)} | e^{-i\hat{H}t} | v_k^{(r)} \rangle \\ &= \lim_{V \rightarrow \infty} \sum_{k=0}^{\infty} \sum_{j=0}^{\infty} \frac{1}{Z} c_{jk} e^{-\beta\epsilon_k} e^{-i(\epsilon_j - \epsilon_k)t}, \end{aligned} \quad (2)$$

where  $|v_k^{(l)}\rangle$  and  $|v_k^{(r)}\rangle$  are the left and right twisted vectors for eigen-state  $|\psi_k\rangle$ ,  $c_{jk}$  is the corresponding weight.

It is easily noted that  $f(t)$  at finite temperature contains contributions from all eigen-states of the quantum many-body system  $\hat{H}$ , with a temperature dependent weight factor for different energy level, but  $f(t)$  remains to include contributions from different periodic functions. Hence the quantum phase classification task essentially remains the same (including its possible reference to  $F(t)$ ) as is shown in the Letter for the ground state. At finite temperature, due to thermal excitations to ground state, the temporal behavior will be more complex thus opening up for more interesting possibilities, e.g., to control *time order* phases and to study crossover or driven phase transitions between different time order phases.

## II. TIME ORDER IN A SPIN-1 ATOMIC BEC

For typical interaction parameters of a spin-1 BEC (e.g., of ground state <sup>87</sup>Rb or <sup>23</sup>Na atoms) in a tight trap, spin domain formation is energetically suppressed when the atom number is not too large as spin-dependent interaction strength is much weaker than spin-independent interaction [1–4]. This facilitates a single-spatial-mode approximation

(SMA) by assuming all spin states share the same spatial wave function  $\phi(\mathbf{r})$ , which effectively decouples the spatial degrees of freedom from the spin and results in the following Hamiltonian [2, 5]

$$\hat{H} = \frac{c_2}{2N} \left[ (2\hat{N}_0 - 1) (\hat{N}_1 + \hat{N}_{-1}) + 2 (\hat{a}_1^\dagger \hat{a}_{-1}^\dagger \hat{a}_0 \hat{a}_0 + \text{h.c.}) \right] - p (\hat{N}_1 - \hat{N}_{-1}) + q (\hat{N}_1 + \hat{N}_{-1}), \quad (3)$$

for the model many body system, where  $\hat{a}_{m_F}(m_F = 0, \pm 1)$  is the annihilation operator of the ground manifold state  $|F = 1, m_F\rangle$  with corresponding number operator  $\hat{N}_{m_F} = \hat{a}_{m_F}^\dagger \hat{a}_{m_F}$ .  $p$  and  $q$  are linear and quadratic Zeeman shifts which could be tuned independently in experiments [6], while  $c_2$  denotes spin exchange interaction strength. The total particle number operator  $\hat{N} = \hat{N}_1 + \hat{N}_0 + \hat{N}_{-1}$  as well as the longitudinal magnetization operator  $\hat{F}_z = \hat{N}_1 - \hat{N}_{-1}$  are both conserved. Thus, linear Zeeman shift can be set to  $p = 0$  effectively.

As discussed in the main text, a suitable order parameter for this model system is  $\hat{n}_{\text{sum}} \equiv \hat{N}_{\text{sum}}/N$  ( $\hat{N}_{\text{sum}} = \hat{N}_1 + \hat{N}_{-1} = N - \hat{N}_0$ ), which measures the fractional atomic population in the states  $|1, 1\rangle$  and  $|1, -1\rangle$  and  $N$  assumes the role of system size. Following our formulation and denoting the system energy eigen-state by  $|\psi_i\rangle$  ( $i = 0, 1, 2, \dots$ ) with increasing eigen-energy  $\epsilon_i$ , the ground state twisted vector becomes  $|v\rangle \equiv \hat{n}_{\text{sum}}|\psi_0\rangle = \sum_{i=0}^{\infty} a_i |\psi_i\rangle$ , with  $a_i = \langle \psi_i | v \rangle$  its expansion coefficient on the eigen-state  $|\psi_i\rangle$ . We find

$$f(t) = \lim_{N \rightarrow \infty} \langle \hat{n}_{\text{sum}}(t) \hat{n}_{\text{sum}}(0) \rangle = \lim_{N \rightarrow \infty} \sum_{j=0}^{\infty} b_j e^{-i(\epsilon_j - \epsilon_0)t}, \quad (4)$$

where  $b_j \equiv |a_j|^2$  is the weight of the ground state twisted vector,  $b \equiv \sum_{j=0}^{\infty} b_j$  the total weight, and

$$F(t) = \lim_{N \rightarrow \infty} \langle \hat{N}_{\text{sum}}(t) \hat{N}_{\text{sum}}(0) \rangle = \lim_{N \rightarrow \infty} \sum_{j=0}^{\infty} B_j e^{-i(\epsilon_j - \epsilon_0)t}, \quad (5)$$

where  $A_i = N \langle \psi_i | v \rangle$ ,  $B_j \equiv |A_j|^2$  is the weight of the enlarged ground state twisted vector, and  $B \equiv \sum_{j=0}^{\infty} B_j$  the total weight.

Our study below is for the zero magnetization  $F_z = 0$  subspace and employs exact diagonalization (ED) to calculate eigen-states as well as eigen-energies. The overall time order phase diagram for spin-1 BEC is shown in the main Letter. For ferromagnetic interaction  $c_2 < 0$ , the critical quadratic Zeeman energy  $q/|c_2| = 2$  splits the whole region into time trivial order (TT) phase for smaller  $q$  that observes TTS, and the generalized time crystalline (gTC) order phase for  $q/|c_2| > 2$  where TTS is spontaneously broken. The latter (gTC phase) is found to coincide with the ground state polar phase. The available computation resource limits the calculation to a finite system size, which prevents us from mapping out the exact details in the immediate neighborhood of  $q = 2$ , where further elaboration is need for its time order properties. On the other hand, for antiferromagnetic interactions, we find  $q = 0$  separates TT phase from and gTC order.

In Figure 1, the weights for the ground state as well as for the low-lying excited states are shown as functions of  $q$  for a typical system size of  $N = 10000$ . Only the ground state weight  $b_0$  is nonvanishing in the  $q < 2$  ( $q < 0$ ) region for ferromagnetic (antiferromagnetic) interactions, but the total weight  $b$  is zero in the  $q > 2$  ( $q > 0$ ) region for ferromagnetic (antiferromagnetic) interaction, which prompts us to examine further the enlarged weights  $B_i$  corresponding to the bulk order parameter. For ground and the first excited states, the volume enlarged weights  $B_{0,1}$  are found to be nonvanishing, although both decrease as  $q$  increases and grow with  $N$  as  $q$  approaches  $q = 2$  ( $q = 0$ ) for ferromagnetic (antiferromagnetic) interaction. However, as mentioned above, limited to a system size of  $N = 10000$  by computation resource in the ED calculation, we cannot exactly map out the behavior near  $q = 2$  ( $q = 0$ ) for ferromagnetic (antiferromagnetic) interaction. This consequently leaves empty for  $q$  in region  $[2.0, 2.02]$  ( $[0, 0.01]$ ) for ferromagnetic (antiferromagnetic) interaction.

The dependence on system size  $N$  is clearly revealed by Fig. 2, with the enlarged weights in the gTC regime attain fixed values as system approaches thermodynamic limit ( $N \rightarrow \infty$ ). In regions away from  $q = 2$  ( $q = 0$ ) for ferromagnetic (antiferromagnetic) interaction, ED numerics can always approach thermodynamic limit except for the immediate neighbourhood near  $q = 2$  ( $q = 0$ ), where we infer with confidence the tendencies to divergence of the weights  $B_{0,1}$  as  $q$  approaches  $q = 2$  ( $q = 0$ ).

The time evolution of two-time auto-correlation function  $F(t)$  is plotted in Fig. 3 (a) for ferromagnetic and (c) for antiferromagnetic interactions, while Figs. 3 (b) and (d) display energy gaps between ground and the first excited states as a function of  $q$  for ferromagnetic and antiferromagnetic interactions respectively at a system size of  $N = 5000$ . The behavior of  $F(t)$  is quantitatively consistent with that of the weights  $B_i(q)$  ( $i = 0, 1$ ) shown in Fig. 1 and the energy gap  $\epsilon_1 - \epsilon_0$  shown in Figs. 3 (b) and (d).

At finite temperature, excited states come into play by also contributing to the correlation function. We find the gTC order hosted in the polar phase persists for both ferromagnetic and antiferromagnetic interactions. The corresponding

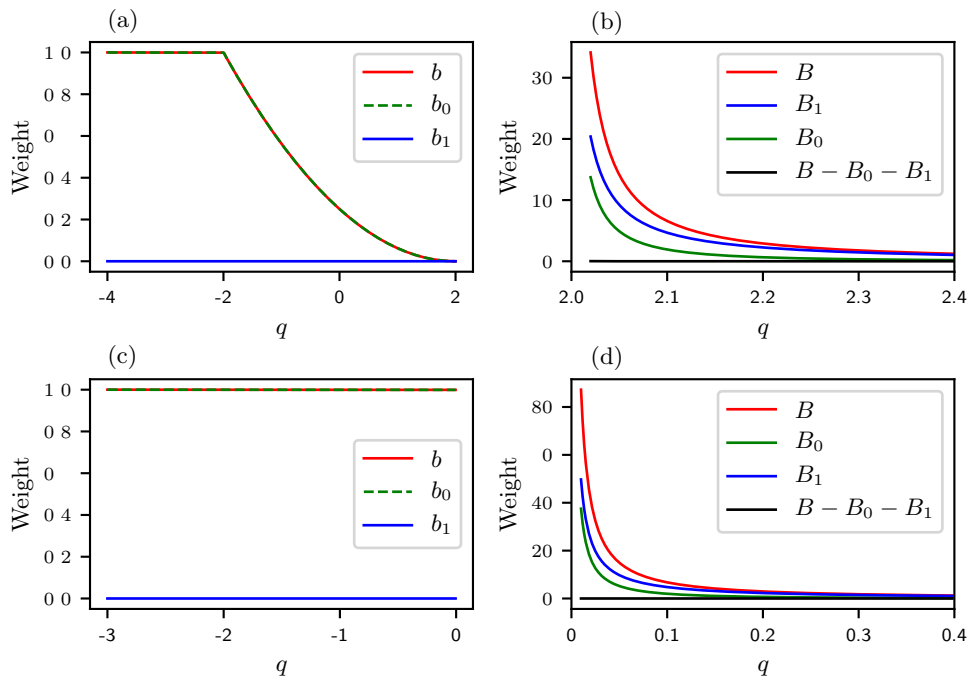


FIG. 1. Weights of ground state twisted vector in the ground and low-lying excited states as functions of  $q$  at system size  $N = 10000$ . The upper panel is for ferromagnetic interaction, where weights  $b_i$  for  $q < 2$  are shown in (a) while weights  $B_i$  for  $q > 2$  are shown in (b). The lower panel is for antiferromagnetic interaction, where weights  $b_i$  for  $q < 0$  are shown in (c) while weights  $B_i$  for  $q > 0$  are shown in (d).

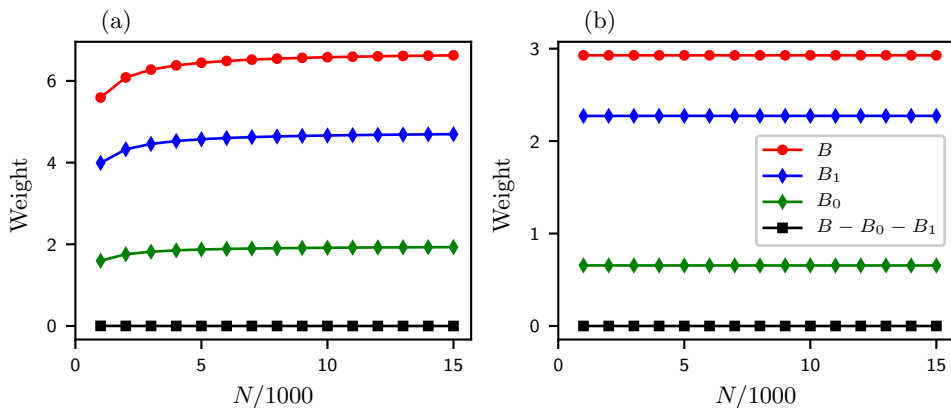


FIG. 2. Weights of ground state twisted vector in the ground and low-lying excited states as functions of system size  $N$  at  $q = 2.1$  for ferromagnetic interaction (a) and at  $q = 0.2$  for antiferromagnetic interaction (b).

time evolution and Fourier transform of  $F(t)$  are shown in Fig. 4, calculated for  $N = 500$  at a temperature of  $\beta \equiv 1/T = 1$ . The Fourier transform is performed for  $\text{Re}(F)$  over  $t = [0, 1000]$  with the zero frequency (DC) component subtracted or for  $\text{Im}(F)$ . The upper (lower) panel corresponds to ferromagnetic (antiferromagnetic) interaction at  $q = 3$  ( $q = 2$ ). For ferromagnetic interaction, two distinct frequency components are clearly identified for  $q = 3$ , associated with the two different energy level gaps. Thus, the gTC phase remains at finite temperature. Moreover, we also find a generalized time quasi-crystalline order phase assuming the two frequencies are incommensurate, by fine tuning their corresponding energy gaps such that the relation  $\Delta_1/\Delta_2 = m_1/m_2$  with  $m_1$  and  $m_2$  being co-primes is not satisfied. The gTC phase at finite temperature here is robust which is in contrast to the melting behavior of Continuous Time Crystal (CTC) shown in Ref. [7].

Finally, we hope to address the critical question about how could this time order, sort of a perpetual time dependence, can be observed. We note the bulk two-time auto-correlation function introduced  $F(t) =$

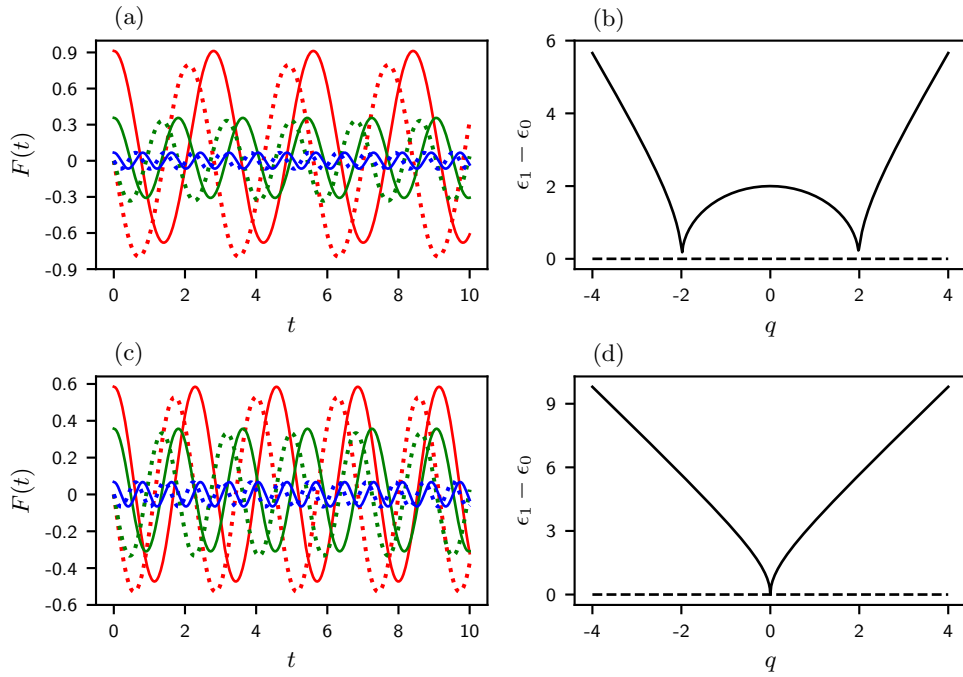


FIG. 3.  $F(t)$  for different  $q$  as a function of time  $t$ . The solid and dotted lines correspond to  $\text{Re}(F)$  and  $\text{Im}(F)$  respectively. The red, green, and blue lines correspond to  $q = 2.5$ ,  $q = 3$ , and  $q = 5$  respectively for ferromagnetic interaction (a). The red, green, and blue lines correspond to  $q = 0.7$ ,  $q = 1$ , and  $q = 3$  respectively for antiferromagnetic interaction (c). The energy gap between ground and the first excited state  $\epsilon_1 - \epsilon_0$  as a function of  $q$  for ferromagnetic (b) and antiferromagnetic interactions (d), at system size  $N = 5000$ .

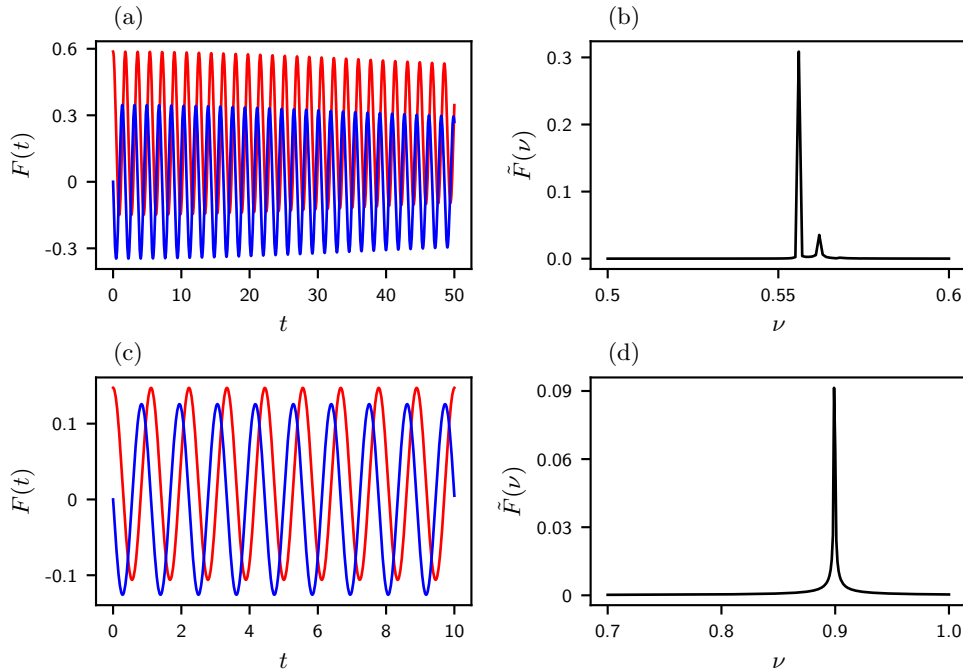


FIG. 4.  $F(t)$  as a function of time  $t$  at  $q = 3$  for ferromagnetic interaction (a) and  $q = 2$  for antiferromagnetic interaction (c). The red and blue solid lines respectively correspond to  $\text{Re}(F)$  and  $\text{Im}(F)$ . The Fourier transform spectrum  $\tilde{F}(\nu)$  of  $\text{Re}(F)$  or  $\text{Im}(F)$  with  $\nu = 1/T$  the frequency,  $T$  the period, for ferromagnetic (b) and antiferromagnetic (d) interactions, at temperature  $\beta = 1$  and system size  $N = 500$ .

$\lim_{N \rightarrow \infty} \langle \hat{N}_{\text{sum}}(t) \hat{N}_{\text{sum}}(0) \rangle$  denotes nothing but the ground state (averaged) conditional outcome of measuring  $N_{\text{sum}}(t)$  at  $t$  after starting with  $N_{\text{sum}}(0)$  initially. The dynamics of  $F(t)$  follows that of  $N_{\text{sum}}(t)$  as in quantum regression theorem. Given the system is well controlled, highly reproducible, one can simply detect  $F(t)$  by measuring  $N_{\text{sum}}(t)$ , although for each measurement at an instant  $t$ , a condensate is destroyed, and a follow up one will have to be prepared as closely as possible in every respects (through selection and post-selection) and be measured at a different  $t' > t$ . Thus, a plausible way to detecting the ground state time dependence will require reconstructing the time dependence of  $F(t)/N_{\text{sum}}(0)$ . As long as the oscillation amplitude is more than a few percent, it will be easily observable with not too much difficulty, although such a reconstruction will still be difficult as  $N_{\text{sum}}(0)$  can be rather small compared to  $N_0 \sim N$  in the polar state. Alternatively, one can perhaps start from a twin-Fock state, i.e., by preparing an initial state with  $N_{\text{sum}}(0) \sim N$ .

In Figure 5(a) we show the behavior of oscillation amplitude for  $F(t)/N_{\text{sum}}(0)$ . The time dependence of  $F(t)/N_{\text{sum}}(0)$  at  $q = 2.5$  for ferromagnetic interaction is shown in Fig. 5(b).

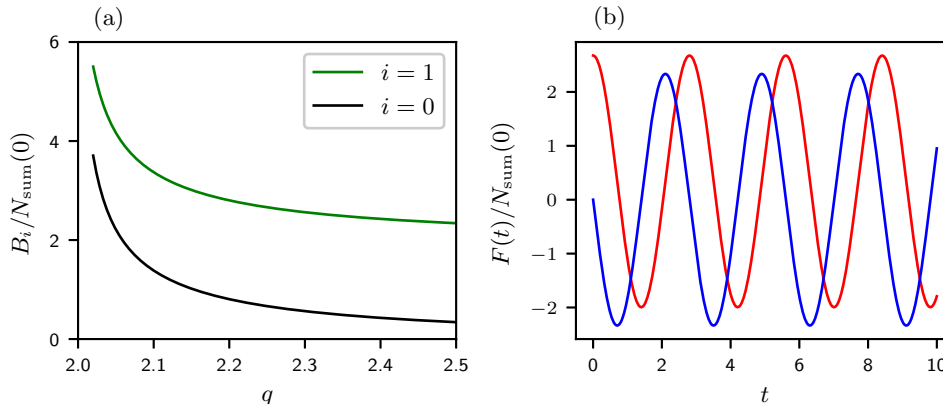


FIG. 5. (a)  $B_i/N_{\text{sum}}(0)$  as a function of  $q$  for ferromagnetic interaction. (b)  $F(t)/N_{\text{sum}}(0)$  as a function of time  $t$  at  $q = 2.5$  for ferromagnetic interaction. The red and blue solid lines correspond to the real and imaginary part of  $F(t)/N_{\text{sum}}(0)$  respectively.

### III. A VARIATIONAL POLAR STATE FOR FERROMAGNETIC SPIN-1 BEC

One might naively expect that nothing particularly interesting could happen in the polar phase of a ferromagnetic spin-1 BEC, where essentially all atoms reside in the single particle state  $|1, 0\rangle$ . Nevertheless, due to the competition between spin exchange interaction  $c_2$  and quadratic Zeeman shift  $q$ , the ground state of our system differs from  $|N_1 = 0, N_0 = N, N_{-1} = 0\rangle$ , which can be affirmed based on a simple variational analytical calculation given in this section.

We use the number state basis  $|N_1, N_0, N_{-1}\rangle \equiv |[N], M, k\rangle$ , where  $N_{m_F}$  denotes occupation number of the  $m_F$  magnetic state,  $M \equiv N_1 - N_{-1}$ , and  $k \equiv N_{-1}$ . We take the following ground state variational ansatz  $|\psi_0\rangle = \frac{1}{\sqrt{1+|a|^2}} (|0, N, 0\rangle + a|1, N-2, 1\rangle)$  for the polar state of ferromagnetic spin-1 BEC, where  $a = re^{i\phi}$  is a (complex) variational parameter with  $r$  and  $\phi$  real. From Eq. (3) and (assumed)  $p = 0$ , the ground state energy follows from

$$\begin{aligned}
 E &= \frac{\langle \psi_0 | H | \psi_0 \rangle}{\langle \psi_0 | \psi_0 \rangle} \\
 &= \frac{1}{1 + a^* a} \left[ \left( \frac{c_2(2N-5)}{N} + 2q \right) a^* a + c_2 \sqrt{\frac{N-1}{N}} (a^* + a) \right] \\
 &= \frac{1}{1 + r^2} \left[ \left( \frac{c_2(2N-5)}{N} + 2q \right) r^2 + 2c_2 \sqrt{\frac{N-1}{N}} r \cos(\phi) \right].
 \end{aligned} \tag{6}$$

We see the extreme value (the minimum) of  $E$  is reached when  $\cos(\phi) = \pm 1$ , i.e., for a real variational parameter  $a$ , which will be assumed from now on. This gives

$$E = \frac{x_1 a^2 + x_2 a}{1 + a^2}, \tag{7}$$

with  $x_1 = \frac{c_2(2N-5)}{N} + 2q$  and  $x_2 = 2c_2\sqrt{\frac{N-1}{N}}$ . The derivative of the energy function  $E(a)$  is

$$E'(a) = \frac{-x_2 a^2 + 2x_1 a + x_2}{(1+a^2)^2}, \quad (8)$$

which determines the locations for the extreme values

$$a_{\pm} = \frac{1}{2c_2\sqrt{N(N-1)}} \left[ c_2(2N-5) + 2Nq \pm N\sqrt{\frac{c_2^2(8N^2-24N+25)}{N^2} + \frac{4c_2q(2N-5)}{N} + 4q^2} \right], \quad (9)$$

and the corresponding extreme values are

$$E_{\pm} = c_2 + q \pm \frac{1}{2}\sqrt{4q^2 + 8c_2q + 8c_2^2 + \frac{-24c_2^2 - 10c_2q}{N} + \frac{25c_2^2}{N^2} - \frac{5c_2}{2N}}. \quad (10)$$

In the thermodynamic limit  $N \rightarrow \infty$ , they reduce respectively to  $a_{\pm} = 1 + \frac{q}{c_2} \pm \frac{\sqrt{2c_2^2 + 2c_2q + q^2}}{c_2}$  and  $E_{\pm} = c_2 + q \pm \sqrt{2c_2^2 + 2c_2q + q^2}$ . The left and right asymptotic value for the energy function  $E(a)$  is therefore

$$E(a) = c_2\left(2 - \frac{5}{N}\right) + 2q, \quad (\text{when } a \rightarrow \pm\infty). \quad (11)$$

For ferromagnetic interaction ( $c_2 < 0$ ),  $E_-$  assumes the minimum, which corresponds to the ground state  $|\psi_0\rangle = \frac{1}{\sqrt{1+a_-^2}} (|0, N, 0\rangle + a_-|1, N-2, 1\rangle)$  with  $N_{\text{sum}} = 2a_-^2/(1+a_-^2)$ , and  $a_- = 1 + \frac{q}{c_2} - \frac{\sqrt{2c_2^2 + 2c_2q + q^2}}{c_2}$  in the thermodynamic limit  $N \rightarrow \infty$ .

Despite of the vanishing order parameter  $n_{\text{sum}}$  in the polar phase (here the gTC order phase from the time order perspective), the enlarged quantity  $N_{\text{sum}}$  retains a finite value. Hence, the physics we present here clearly belongs to the realm of quantum effects, beyond the reach of mean-field theory.

#### IV. THE NON-HERMITIAN SPIN MODEL WITH MULTI-BODY INTERACTION

The non-Hermitian quantum many body model Hamiltonian is

$$\hat{H} = \hat{H}_0 + (\lambda + \gamma i)\hat{H}_1, \quad (12)$$

with

$$\begin{aligned} \hat{H}_0 &= -\sum_{j=1}^N \sigma_j^z \sigma_{j+1}^z, \\ \hat{H}_1 &= \sigma_1^x \sigma_2^x \cdots \sigma_{[N/2]}^x - \sigma_{[N/2]+1}^x \cdots \sigma_N^x, \end{aligned} \quad (13)$$

where  $[\cdot]$  denotes the integral part,  $\sigma_{N+1} \equiv \sigma_1$ ,  $\lambda$  and  $\gamma$  are spin-string interaction strength and dissipation strength respectively.  $\lambda$  and  $\gamma$  are both real numbers.  $i$  is the imaginary unit.  $\sigma^{x,y,z}$  are Pauli operators.  $N$  is the qubit number of the system. The Hamiltonian has the  $[(N+1)/2]$ -body interaction term and supports the GHZ state  $|G_+\rangle$  as a non-degenerate excited state.

Firstly, denote the Greenberger-Horner-Zeilinger (GHZ) states as

$$|G_{\pm}\rangle = \frac{1}{2}(|0\rangle^{\otimes N} \pm |1\rangle^{\otimes N}). \quad (14)$$

Denote

$$|\tilde{G}_{-, \mathcal{I}}\rangle = \frac{1}{\sqrt{2}} (|0\rangle_1 \cdots |0\rangle_{[N/2]} |1\rangle_{[N/2]+1} \cdots |1\rangle_N - |1\rangle_1 \cdots |1\rangle_{[N/2]} |0\rangle_{[N/2]+1} \cdots |0\rangle_N), \quad (15)$$

where  $\mathcal{I} = ([N/2] + 1, [N/2] + 2, \dots, N)$  is a multi-index.

We immediately know that  $|G_{\pm}\rangle$  are the degenerate ground state of the ferromagnetic Ising Hamiltonian  $\hat{H}_0$  with

eigen-energy  $E_{(0)} = -N$ ,  $|\tilde{G}_{-, \mathcal{I}}\rangle$  is the excited state of  $\hat{H}_0$  with eigen-energy  $E_{(1)} = -N + 4$ .

The action of  $\hat{H}_1$  on  $|G_{-}\rangle$  ( $|\tilde{G}_{-, \mathcal{I}}\rangle$ ) gives  $|\tilde{G}_{-, \mathcal{I}}\rangle$  ( $|G_{-}\rangle$ ) with a multiplicative factor  $-2$ .

$$\begin{aligned}\hat{H}_1|G_{-}\rangle &= -2|\tilde{G}_{-, \mathcal{I}}\rangle, \\ \hat{H}_1|\tilde{G}_{-, \mathcal{I}}\rangle &= -2|G_{-}\rangle.\end{aligned}\tag{16}$$

Then we know the two eigen-states of  $\hat{H}$  is a superpositon of  $|G_{-}\rangle$  and  $|\tilde{G}_{-, \mathcal{I}}\rangle$  and can be written as

$$|\Psi\rangle = \alpha_1|G_{-}\rangle + \alpha_2|\tilde{G}_{-, \mathcal{I}}\rangle,\tag{17}$$

where  $\alpha_{1,2}$  are the undetermined coefficients. Substitute into the Schrödinger equation  $\hat{H}\Psi = \epsilon|\Psi\rangle$ , we get

$$\epsilon^2 - (E_{(0)} + E_{(1)})\epsilon + (E_{(0)}E_{(1)} - 4(\lambda + \gamma i)^2) = 0,\tag{18}$$

$$2(\lambda + \gamma i)\alpha_2 = (E_{(0)} - \epsilon)\alpha_1.\tag{19}$$

The eigen-energy  $\epsilon^{(\pm)} = \frac{1}{2}[E_{(0)} + E_{(1)} \pm \sqrt{(E_{(1)} - E_{(0)})^2 + 16(\lambda + \gamma i)^2}]$ . Choose  $\alpha_1 = 1$ , we have  $\alpha_2 = \frac{E_{(0)} - \epsilon}{2(\lambda + \gamma i)}$ . Imposing the normalization condition, we have

$$|\Psi^{(\pm)}\rangle = \frac{\alpha_1}{\sqrt{|\alpha_1|^2 + |\alpha_2|^2}}|G_{-}\rangle + \frac{\alpha_2}{\sqrt{|\alpha_1|^2 + |\alpha_2|^2}}|\tilde{G}_{-, \mathcal{I}}\rangle.\tag{20}$$

If  $\gamma = 0$ , the Hamiltonian is Hermitian and we have the ground state  $|\Psi_0\rangle \equiv |\Psi^{(-)}\rangle$  with energy  $\epsilon_0 \equiv \epsilon^{(-)} = -N - 2(\sqrt{1 + \lambda^2} - 1)$ . See more details about the Hermitian version of the system in Ref. [8]. Here, we choose the eigen-state from  $\{|\Psi^{(+)}\rangle, |\Psi^{(-)}\rangle\}$  as the ground state  $|\Psi_0\rangle$  of our generalized non-Hermitian system, for it deforms into the ground state of the Hermitian case when  $\gamma$  approaches zero. If  $\epsilon$  is real, then the ground state energy  $\epsilon_0$  corresponds to the smaller one from  $\epsilon^{(\pm)}$ . However, the ground state energy  $\epsilon_0$  corresponds to the one with the larger imaginary part when  $\epsilon$  is a complex number. The ground state  $|\Psi_0\rangle$  are obtained straightforwardly.

For the GHZ state  $|G_{+}\rangle$ , we can know it's a non-degenerate excited state with energy  $\epsilon_{+} = -N$ , for

$$\hat{H}_1|G_{+}\rangle = 0.\tag{21}$$

- 
- [1] T.-L. Ho, *Phys. Rev. Lett.* **81**, 742 (1998).
  - [2] C. K. Law, H. Pu, and N. P. Bigelow, *Phys. Rev. Lett.* **81**, 5257 (1998).
  - [3] M. Koashi and M. Ueda, *Phys. Rev. Lett.* **84**, 1066 (2000).
  - [4] D. M. Stamper-Kurn and M. Ueda, *Rev. Mod. Phys.* **85**, 1191 (2013).
  - [5] H. Pu, C. K. Law, S. Raghavan, J. H. Eberly, and N. P. Bigelow, *Phys. Rev. A* **60**, 1463 (1999).
  - [6] X.-Y. Luo, Y.-Q. Zou, L.-N. Wu, Q. Liu, M.-F. Han, M. K. Tey, and L. You, *Science* **355**, 620 (2017).
  - [7] V. K. Kozin and O. Kyriienko, *Phys. Rev. Lett.* **123**, 210602 (2019).
  - [8] P. Facchi, G. Florio, S. Pascazio, and F. V. Pepe, *Phys. Rev. Lett.* **107**, 260502 (2011).